

**QUANTIFYING THE IMPACT OF SHIP GENERATED WAVES
ON PEA PATCH ISLAND**

by

Mike Larner

A thesis submitted to the Faculty of the University of Delaware in partial fulfillment of the requirements for the degree of Bachelor of Civil Engineering with Distinction

Spring 2019

© 2019 Mike Larner
All Rights Reserved

**QUANTIFYING THE IMPACT OF SHIP GENERATED WAVES
ON PEA PATCH ISLAND**

by

Mike Lerner

Approved: _____
Jack A Puleo, Ph.D.
Professor in charge of thesis on behalf of the Advisory Committee

Approved: _____
Thomas McKenna, Ph.D.
Committee member from the Department of Geological Sciences

Approved: _____
Sue McNeil, Ph.D.
Committee member from the Board of Senior Thesis Readers

Approved: _____
Michael Chajes, Ph.D.
Chair of the University Committee on Student and Faculty Honors

ACKNOWLEDGMENTS

First and foremost, I would like to thank my friends and family for their unconditional support and patience throughout my educational experience. I cannot begin to express how much I appreciate all the hours dedicated to pretending to know what I was talking about whenever I would discuss my research, and for always having my back when I would get in long winded arguments with MATLAB.

Furthermore, I would like to thank the amazing team of dedicated students who made the weekly journey to Pea Patch Island and battled the heat, mud, and bugs during their summer break to assist in this project. I could not have completed this project without the help of Stan, Ben, Maro, Rory, and Demi; all of you have helped me tremendously with finding missing semicolons and retrospectively obvious syntax errors in my codes. A special thanks goes out to Rachel Schaefer, who has worked alongside me with this project since the beginning and has been a great resource for advice as well as always being there to listen to my complaints.

Additionally, I would like to acknowledge the support I received from the University of Delaware for awarding me a fellowship and providing conference funding for registration fees and travel expenses to present my research. Without this help I would not have been able to complete this project. I am also grateful for the support of the Delaware Department of Natural Resources and Environmental Control (DNREC) for providing access to Pea Patch Island and the use of their crew boat to transport all of our equipment.

I would like to thank my committee for all your time and supportive suggestions. Dr. Tom McKenna, thank you for your help in the field, even if Pea Patch Island isn't what most would consider paradise, I would still "rather be in a boat with a drink on the rocks, than in the drink with a boat on the rocks." Thank you, Dr. Sue McNeil, for helping with my presentation introduction and all your guidance throughout the year. Last, but most certainly not least, I would especially like to thank my advisor, Dr. Jack A Puleo. Although there may have been times where pointing out the answer to my questions and explicitly telling me what to do would have saved you a lot of time and frustration, I am extremely grateful for all the *carte blanche* you have given me; allowing me to connect the dots and discover answers on my own.

TABLE OF CONTENTS

LIST OF TABLES	vi
LIST OF FIGURES.....	vii
ABSTRACT	x
1 INTRODUCTION.....	1
1.1 Motivation	3
2 FIELD STUDY	6
2.1 Study Site.....	6
2.2 Methods	7
2.2.1 Instrumentation.....	10
2.2.1.1 Electro-Magnetic Current Meters.....	11
2.2.1.2 Pressure Sensors	12
2.2.1.3 Acoustic Distance Meters (ADM).....	13
2.2.1.4 Real-Time Kinematic GPS.....	15
2.2.1.5 Time-Lapse Camera	17
2.2.2 Data Analysis.....	18
2.2.2.1 Time Series Analysis.....	22
2.2.2.2 Automatic Identification System (AIS) Data	23
3 RESULTS.....	25
3.1 Wake Characteristics	25
3.2 Geomorphological Change	27
3.3 Energy Flux	29
4 CONCLUSIONS AND FUTURE WORK.....	35
REFERENCES.....	37

LIST OF TABLES

Table 3.1	Average energy flux per ship and average ambient energy flux during a 15-minute period.....	33
-----------	---	----

LIST OF FIGURES

Figure 1	Geographic location of Pea Patch Island (<i>Maps obtained from Google Earth</i>).....	2
Figure 2	Flowchart depicting the method in which the data were processed and analyzed. A frequency domain analysis approach was used initially, however, it was decided that a time domain analysis was more practical.	5
Figure 3	(a) Pea Patch Island, 1) Study site location. 2) Fort Delaware. 3) Stone embankment constructed to stabilize the shoreline surrounding the fort. 4) Shipping channel. (b) Local bathymetry of waters surrounding Pea Patch Island (<i>Image courtesy of NOAA nautical chart 12311</i>). Soundings in feet.	7
Figure 4	Stations M0 – M6 labeled on the transect at the study site. Due to the proximity from one another, stations M3 and M4 are not labeled in the figure.	9
Figure 5	Stations M1-M5 set up along the transect. Stations M3, M4, and M5 are stabilized by an additional vertical pipe on the left side of the transect. Station M0 is not visible in the figure because it was submerged at the time this picture was taken.	10
Figure 6	JFE at station M3 positioned 0.1 m above the bed. The JFEs at stations M4 and M5 can be seen in the background.....	12
Figure 7	RBR Solo hydrostatic pressure sensor, contains an internal power supply and self-storage for self-contain in situ deployments.	13
Figure 8	Front and back view of the Banner T30 ADM sensor. This image does not include the data logger or battery that were connected to the ADM for the field study.	14
Figure 9	ADM connected to the Lithium Polymer battery and data logger in the weather proof box.....	15
Figure 10	GNSS RTK GSP surveying along the submerged region of the transect. The orientation of this picture is looking towards the main channel from the dry beach along the study site transect. (<i>Picture taken by Evan Krape</i>).	16

Figure 11	Time lapse imagery captured June 26, 2018. (a) Ship travelling south approaches study site at 9:37:10 am, (b) drawdown transitioning to incoming surge at 9:39:10 am, (c) maximum shoreward extent of surge runup has been met and remaining wave energy is reflected offshore at 9:39:40 am, (d) higher frequency divergent wake train propagates towards shore at 9:40:10 am.	17
Figure 12	Unfiltered RBR data from the evening on June 8th overlain on the tidal trend that was developed by using a 30-minute moving average. ..	19
Figure 13	RBR data filtered with a Savitzky-Golay convolution filter plotted with unfiltered RBR data and tidal trend during the evening of June 8 th	20
Figure 14	(a) Time series of a 24-hour segment of low frequency filtered data before the tidal trend was removed. (b) Same filtered data with the tidal trend removed and individual event extrema identified (the extrema are plotted in absolute magnitude).	22
Figure 15	Relative water level plotted over time of low frequency oscillations generated by 189 ships that passed by the study site from June 7 th to July 9 th	26
Figure 16	Low frequency signals of 8 ships traveling during a similar tide phase. (a) Ships traveling south past Pea Patch Island. (b) Ships traveling north past Pea Patch Island.....	27
Figure 17	Wind rose of wind speed and direction from June 7, 2108 to July 9, 2018. <i>Data obtained National Data Buoy Center (NDBC) Station DELD1 (Delaware City).</i>	28
Figure 18	During the field study 8 profile surveys were conducted and plotted together to compare the temporal variations over the duration of the study. The legend identifies the each of the colored curves with the corresponding date of the survey.....	29
Figure 19	Percent of average daily energy flux contributed by identified ships compared to the total daily energy flux experienced at each station along the transect.....	31
Figure 20	Averaged total daily energy flux recorded at Stations M0 – M4 compared to the averaged daily energy flux contributed by the wake events identified in the RBR pressure data.	32

Figure 21 Energy Flux recorded across the transect of 3 randomly selected ships.
An increase in energy flux can be observed as the waves move
landward toward shallower water and then rapidly dissipate after
breaking 34

ABSTRACT

Waterways such as rivers, canals, and estuarine shipping lanes are not naturally well defended against large wave events because they are subjected primarily to currents, tides, and small wind waves. Large waves are uncommon in these environments due to the relatively narrow fetch and shallow bathymetry. However, increasing human activity as well as the growth of trade and commerce has introduced the necessity to further research to investigate the impacts associated with large vessel generated waves. Repetitive wave forces generated by large vessels traveling through narrow and shallow channels can disrupt the natural morphology of nearby beaches and river banks.

The goal of this research project is to evaluate the hydrodynamic characteristics of ship generated waves and quantify the relative impact of ship generated wave events on Pea Patch Island in New Castle County, Delaware. To perform this analysis, a month-long instrumented field study was conducted on the shoreline of Pea Patch Island adjacent to the main shipping channel of the Delaware River. The data collected in the study were used to inspect the energy transferred from individual wake events caused by passing ships and compare with the energy associated with ambient bay conditions.

Chapter 1

INTRODUCTION

Pea Patch island (39°35.67'N, 75°34.35'W), located in the Delaware River, is a river silt deposit formed island. The island sits off the coast of Delaware city and is equidistant from the Delaware and New Jersey shorelines (Figure 1). Pea Patch Island is a low-lying island with a maximum natural elevation of approximately 3 m. Much of the island is comprised of marshy wetlands due to its low elevation and muddy composition, making it susceptible to inland flooding during increased river levels. Although the salinity in this region of the river is negligible, the water level is still strongly influenced by lunar tide phases. Natural sediment transport in tidal waterways is affected by the tidal range and controls the development and erosion of marshes and shorelines (Ross et al., 2017). The spatial and botanical variation in these waterways are directly influenced by the energy intensity commonly experienced. Inherently, high energy areas consist of more coarse grain sediment and are prone to being less vegetated due finer sediments having a lower settling velocity and plants unable to take root.

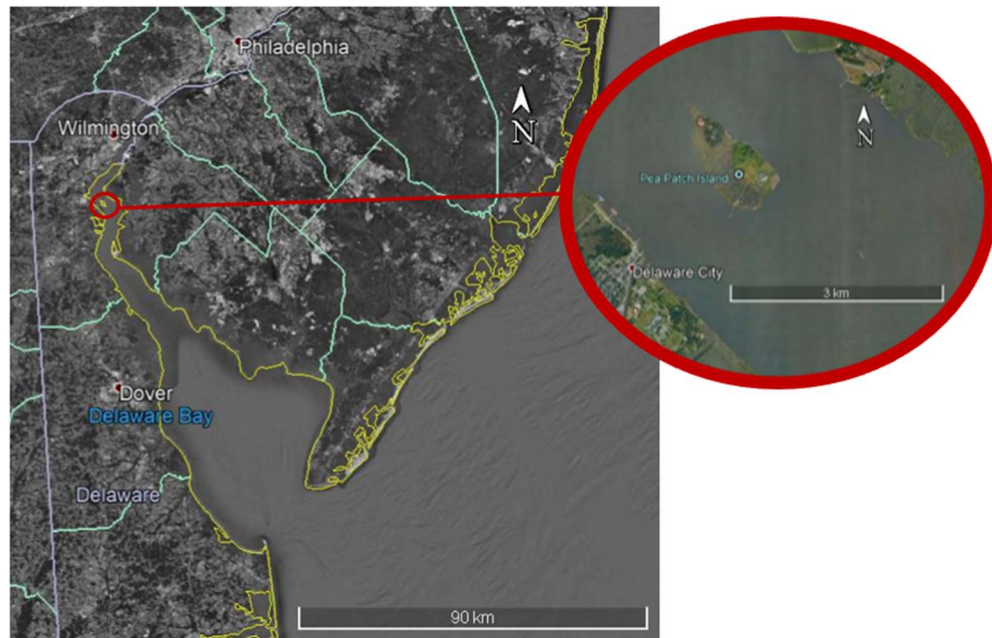


Figure 1 Geographic location of Pea Patch Island (*Maps obtained from Google Earth*).

The impacts of tides are increased in the Delaware River and Bay system due to the converging geometry of the coastlines creating strong frictional and fluvial effects (Parker, 1984). Yet, Pea Patch Island shorelines vary from non-vegetated sandy sloped beaches to densely vegetated peat platforms. It is assumed that this botanical dissimilarity is caused by the difference in hydrodynamic energy at varying locations along the island's shoreline. The non-vegetated beaches on the island are primarily located on the northeast side of the island adjacent to the main shipping channel and, per contra, the vegetated shorelines face the shallower, less travelled, southwest side of the island.

1.1 Motivation

The Delaware River is one of the most commercially navigated waterways in the East Coast. It has over 40 ports and anchorages with about 3000 visiting ships each year, supplying and exporting goods from major cities such as Camden, Philadelphia, Wilmington, and Trenton (Almaz & Altiok, 2012). Dredging projects have been in progress since 2002 to increase the channel depth to 15 m in an effort to accommodate larger vessels and increasing shipping traffic (Cook et al., 2007). Pea Patch Island is home to the historic Fort Delaware as well as an established breeding ground for migratory wading bird colonies and is threatened by increased human activity and rising sea levels.

While shorelines are dynamic protection mechanisms for inland areas, a rising concern is whether the Island will be able to adapt fast enough to the acceleration of external forces impacting its coast. Shoreline retreat and cross-shore sediment transport are an indication of a beach's effort in decreasing the foreshore slope to better dissipate wave driven forces acting on the beach (Dean & Dalrymple, 2004). However, the continuous dredging of the Delaware River channel decreases frictional forces and increases tidal amplitude resulting in higher alongshore currents (Kjerfve, 2018). The increase in alongshore currents removes the suspended sediment from the local system. Furthermore, a stone embankment was constructed along the edge of the island south of the study site to stabilize the shoreline surrounding the Fort to inhibit the Island's shoreline retreat and provide protection from overtopping due to waves and extreme tides. Conversely, the embankment impedes alongshore sediment transport upriver, and recent observations have shown scarping of the shoreline on the northern and southern ends of the embankment facing the main channel. The lack of alongshore sediment transport creates a discontinuity forcing sediment to be eroded

from the beach at the study site (Komar, 1998). The increased rate of erosion without a downriver sediment supply disrupts the natural coastal process's ability to keep pace with changes needed to adapt to sea level rise and increased shipping traffic.

The primary goal of this research is to quantify the impact of ship generated wakes on Pea Patch Island by examining the relationship of wake induced energy fluxes and ambient river conditions. In the following chapters, a description of the study site, along with an explanation of why it was selected, are presented. Subsequently, the data collection methods and instrumentation are discussed with a walk through of the data analysis (Figure 2). Finally, a brief discussion of the results of the analysis is given.

The issues pertaining to the Delaware River are common to many other ports and waterway systems. Thus, the analysis approaches presented herein provide guidelines that can be implemented to other systems.

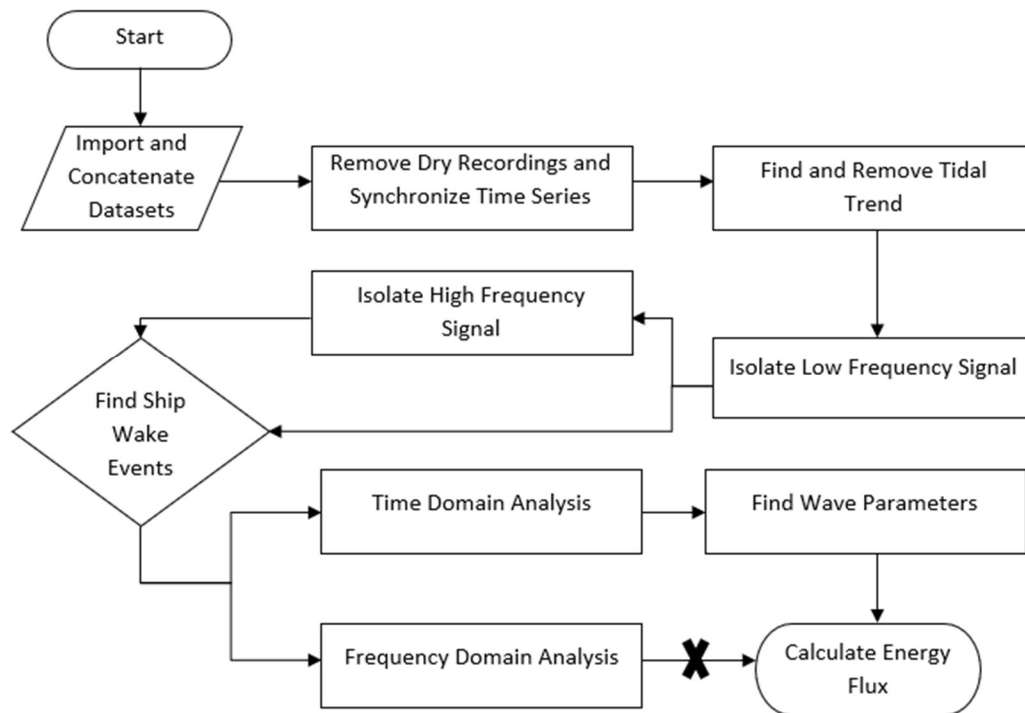


Figure 2 Flowchart depicting the method in which the data were processed and analyzed. A frequency domain analysis approach was used initially, however, it was decided that a time domain analysis was more practical.

Chapter 2

FIELD STUDY

2.1 Study Site

The chosen study site is located on a crescent shaped beach on the northeastern side of the island just beyond the northern end of the stone embankment adjacent to the main shipping channel (Figure 3). The beach in this region of the Island has been eroded into a crenulate bay because a vegetated platform that protrudes from the island towards the shipping channel on the southern end of the beach. The platform acts as a headland at the end of the stone embankment, that shelters the beach from alongshore sediment transport flowing up river. It is important to further understand whether this area of the island is starved from naturally mobilized sediment or if it is escalated by the effects of large vessel disruption, making it an ideal location to measure the energy flux distributed by passing vessels.

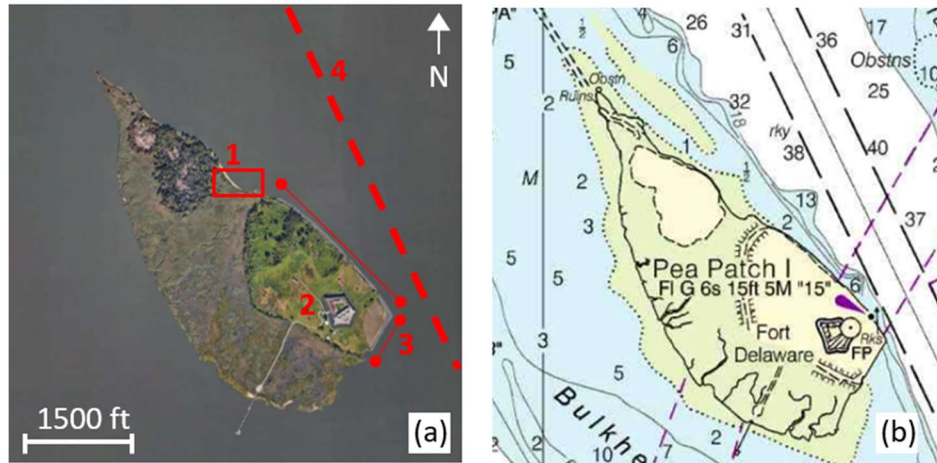


Figure 3 (a) Pea Patch Island, 1) Study site location. 2) Fort Delaware. 3) Stone embankment constructed to stabilize the shoreline surrounding the fort. 4) Shipping channel. (b) Local bathymetry of waters surrounding Pea Patch Island (*Image courtesy of NOAA nautical chart 12311*). Soundings in feet.

2.2 Methods

A study was conducted from June 6 to July 9, 2018 in the littoral zone on the northeastern side of the island adjacent to the main shipping channel to quantify nonlinear wave groups generated by large vessels traveling at subcritical speeds. Using current meters, pressure sensors, and ultrasonic distance meters the near shore velocities and relative wave heights of the wakes and low-frequency oscillations of the wakes from the ships were measured in correlation with current river conditions.

A cross-shore transect was constructed across an unobstructed region of the beach that ran perpendicular to the channel (Figure 4). The transect line was desired to span from below the low-water spring tide line, through the intertidal zone, to the top of the berm; however, due to accessibility constraints the farthest offshore data collection station was above water during the majority of low tides. This was inconsequential as shipping activity was also limited during these times and the

vessels that were traveling past Pea Patch Island at low tides did not generate waves capable of propagating across the entire transect due to low water levels. Currently, the sailing depth of ships is restricted to less than 12 m during low tides causing larger, more heavily loaded, ships to work around the tide or transfer cargo to lightering barges (Almaz & Altiok, 2012).

The transect consisted of six data collection stations labeled from M0 to M5 in ascending order beginning from M0 offshore to M5 located at the top of the berm (Figure 5). Five of the stations (M1 – M5) were secured by using 8- and 12-foot vertical steel pipes, with the 8-foot pipes used on the beach face and the 12-foot pipes driven into silty mud in the foreshore zone. The pipes were driven into the ground using a slide hammer to a depth of approximately 4-5 feet. Due to the silty clay composition of the mud it was postulated that enough frictional resistance acting on the surface area of the pipes would impede additional sinking over the course of the study. As an added measure to ensure no additional sinking would occur, a wooden plate was fastened to the pipe at bed level to act as a footing. The stations located in the muddy foreshore region of the transect were secured from torsional rotation by the addition of steel netting at the base of the pipe to serve as perpendicular support from unbalanced horizontal stresses. The stations located on the beach face were secured from rotation by the addition of a second, smaller, vertical pipe that was driven into the ground next to each of the corresponding stations and connected via the horizontal cross member.

The initial deployment took place on June 6th and 7th, and data collection began on June 7th at 1:30 pm local time. Island access was restricted to Delaware Department of Natural Resources and Environmental Control (DNREC) regular hours of

operation. Site visits were limited to once a week with two intensive studies conducted during the lunar spring tides. During the intensive studies, daily trips to the island were made for observations and sampling rates were increased on the accessible sensors. The sensors and stationing equipment were recovered on July 9th.

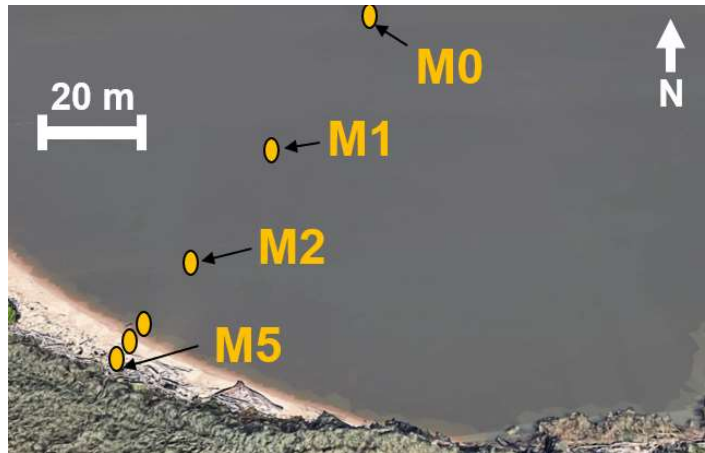


Figure 4 Stations M0 – M6 labeled on the transect at the study site. Due to the proximity from one another, stations M3 and M4 are not labeled in the figure.



Figure 5 Stations M1-M5 set up along the transect. Stations M3, M4, and M5 are stabilized by an additional vertical pipe on the left side of the transect. Station M0 is not visible in the figure because it was submerged at the time this picture was taken.

2.2.1 Instrumentation

In situ measurements of wave height, water depth, fluid velocity and bed level change were collected throughout the duration of this study to quantify the energy fluxes induced by ship wakes relative to the ambient fluvial conditions throughout the duration of this study. To measure these parameters, an assortment of sensors was used in conjunction with internal and external batteries and data loggers that were able to operate independently (self-contained) at various stations across the transect. Using current meters, pressure sensors, and ultrasonic distance meters the near shore velocities and relative wave heights of the transverse and divergent wakes from the ships were measured in conjunction with current bay conditions. A time lapse camera

was also used as a visual component to confirm ships passing with correlated data indicators.

2.2.1.1 Electro-Magnetic Current Meters

Four JFE Advantech electro-magnetic current meters were used to measure and record the variation in horizontal velocities across the transect. The JFEs were chosen due to rugged fabrication and self-contained storage and internal battery. To maximize the battery life of the JFEs, they were set to record on burst mode, sampling at 5 Hz for 3 minutes every 15 minutes. At this setting, it was still necessary to offload the data and replace the batteries after a week of sampling. During the intensive study periods of the project, the JFEs were set to record continuously at 5 Hz. In this setting, the battery life expectation was limited to approximately 4 days. The JFEs were positioned to record the fluid velocity 0.1 m above bed level at stations M1, M3, M4, and M5 (Figure 6). It is worth noting that the JFE at station M5 was used to record velocities at the highest predicted location of inundation on the beach in the event of an extreme situation. However, water levels did not reach 0.1 m depth at station M5 given the conditions during the project. During the weekly visits to the site, the position of the JFEs were re-measured and adjusted in the event that there was any bed level change. The adjustments ensured that the horizontal velocity recordings were measured at a constant elevation throughout the duration of the project.



Figure 6 JFE at station M3 positioned 0.1 m above the bed. The JFEs at stations M4 and M5 can be seen in the background.

2.2.1.2 Pressure Sensors

A fundamental parameter in calculating the energy contained within a wave is the height of the wave being analyzed. To obtain the wave heights generated by passing vessels, it was necessary to measure the instantaneous water height relative to the local bed level. Inherently, small wind-generated waves in sheltered environments tend to have small periods (1-5 seconds), so a minimum sampling frequency of 2 Hz was desired to avoid aliasing. In addition to having an adequate sampling rate, internal power and self-storage were also essential in maintaining consistent depth measurements without having to retrieve the sensors throughout the study. To accommodate these requirements, a mixed array of five RBR Solo pressure sensors (Figure 7) were used at stations M0 – M4 to record and log the hydrostatic water pressure across the transect. An additional pressure sensor was stationed above the

berm on the time-lapse camera pole to record the atmospheric pressure. The RBRs at stations M0, M2, and M3 were able to record data at 16 Hz, and the RBRs at stations M1 and M4 recorded at 2 Hz.

The low power drawing requirements of the RBR enabled them to record for over 30 days if primarily submerged. The battery life of the RBRs at Stations M3 and M4 was reduced by 1 and 2 days respectively, limiting the duration of analyzed data to 30 days. It was believed that this may have been caused the prolonged exposure to sunlight the RBRs experienced at these stations.



Figure 7 RBR Solo hydrostatic pressure sensor, contains an internal power supply and self-storage for self-contain in situ deployments.

2.2.1.3 Acoustic Distance Meters (ADM)

The Acoustic Distance Meters (ADMs) used were Banner T30 ultrasonic sensors (Figure 8). The lightweight design and adjustable window sensing capabilities made the T30 a universal device compatible for use at various station locations across the transect. The ADMs served a dual purpose in measuring both water and bed level change. They were an important resource in cross-referencing findings from the pressure data but were unable to detect very small changes that were not uniform across the width of its sampling window. This lack of precision was due to the width of the sampling window, causing the closest object identified in the field to be

returned. This may have had an effect on not recognizing very small fluctuations in water levels. However, fluctuations in the water level small enough to not be returned in the ADM data were not representative of the ship wake signals.

Additionally, if any substantial bed level change occurred, the ADMs can capture the change more frequently than the project beach profile surveys. The bed level change that is collected using the ADMs is measured between every tide as well as whenever the water level drops below bed level within the sampling frequency. The ADMs were used on site, with 3 of them being located on the beach face ascending from the base of the berm up to the berm crest, the 4th was located at station M2 to measure any possible change in the foreshore region of the transect.



Figure 8 Front and back view of the Banner T30 ADM sensor. This image does not include the data logger or battery that were connected to the ADM for the field study.

The ADMs are not self-storing devices and require an external power source. A MadgeTech data logger was used to store data and a 12 V Lithium Polymer battery was used to power the ADM. A weatherproof box was modified to house and protect the additional devices needed to operate the ADMs (Figure 9). For the ADM to work

correctly without jeopardizing the waterproof integrity of the box, a circular hole was drilled through the bottom of the box to allow an unobstructed path for the sensor to send and receive high frequency signals. The signals were later calibrated in the Center for Applied Coastal Research lab to translate the signal sent and received at a constant distance.

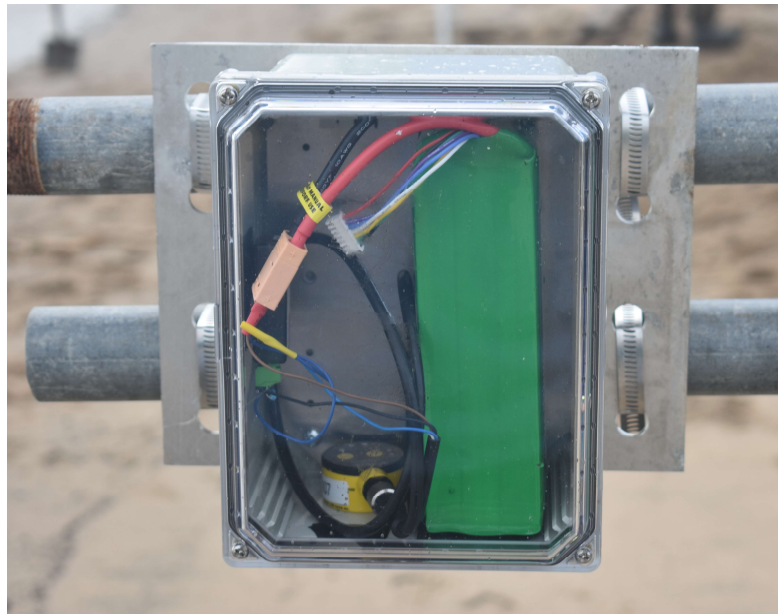


Figure 9 ADM connected to the Lithium Polymer battery and data logger in the weather proof box.

2.2.1.4 Real-Time Kinematic GPS

To measure the temporal geomorphological change during the project, vertical transect profile data were collected using a Leica Global Navigation Satellite System (GNSS) Real Time Kinematic (RTK) Rover GPS. The data were measured from above the swash limit to just seaward of station M0 and were recorded in relation to the North American Vertical Datum of 1988 (NAVD88). The GNSS antenna was

positioned on a 2-meter-long pole to measure the full length of transect including the submerged nearshore regions (Figure 10).

The profile surveys were conducted at low tide during each of the site visits. However, due to tides that were not conducive to the limited site access, some surveys were not able to extend beyond station M0. The effects of this were not appreciable, as there were only minimal variations measured during the different profile surveys.



Figure 10 GNSS RTK GSP surveying along the submerged region of the transect. The orientation of this picture is looking towards the main channel from the dry beach along the study site transect. *(Picture taken by Evan Krape).*

2.2.1.5 Time-Lapse Camera

A time lapse camera was stationed on the upper region of the back beach and positioned offset from the transect to provide time-stamped photo imagery of passing ships and the ship wakes propagating up the beach. The time stamped imagery served a multifunctional purpose by recording both the events and allowing for cross referencing in ship identification. The camera was set to record images every 30 seconds between 5:30 am and 9:00 pm. These parameters were chosen due to daylight hours during the project as well as to optimize the storage and battery life of the camera while still capturing all passing ships throughout the day and the respective events of interest (drawdown, surge, and divergent wake train). The utilization of the time lapse camera is exemplified in Figure 11.



Figure 11 Time lapse imagery captured June 26, 2018. **(a)** Ship travelling south approaches study site at 9:37:10 am, **(b)** drawdown transitioning to incoming surge at 9:39:10 am, **(c)** maximum shoreward extent of surge runup has been met and remaining wave energy is reflected offshore at 9:39:40 am, **(d)** higher frequency divergent wake train propagates towards shore at 9:40:10 am.

2.2.2 Data Analysis

Due to the length of the data collection, many of the sensors required data offloading and battery swaps periodically throughout the course of the study, resulting in multiple datasets that were concatenated and synchronized to the time series recorded by the RBR soloD at station M0. The data acquired from the pressure sensors were adjusted by removing atmospheric influences that were measured using the additional pressure sensor located on the time lapse camera station. After adjusting the pressure data, the measurements were converted to water elevation by reorganizing the hydrostatic pressure equation and solving for depth.

$$d = \frac{P}{\rho g}, \quad (2.1)$$

where g represents the acceleration force due to gravity, P is the hydrostatic pressure, and ρ is the density of water. The density of water was obtained by local buoy data from NOAA Station DELD1 located in Delaware City, and averaged for the duration of the study. It is worth noting that slight variations in water density would result in negligible error in the depth calculation.

The water depth data were then used to quality control the velocity data sets obtained from the JFEs. This process involved eliminating any data that were recorded while the JFE was above water. The JFE sensor at each station was correlated with the corresponding pressure sensor at that station and if the data represented a water level below 0.15 m the data points were removed until a substantial depth measurement was met. The additional five centimeters was included as a conservative measure to ensure that the sensor probe of the JFE was submerged. Data acquired from any ships passing

at these water levels would be unusable anyways, as the troughs from subsequent waves would result in “dry” readings by the JFEs.

Astronomic tidal influences were estimated using a moving average filter with a 30-minute window (Figure 12) and removed by subtracting the tidal trend from the RBR data set. The 30-minute averaging window was chosen because it fit the tidal curve represented in the data without causing discernible averaging of the background noise and ship wakes. Apparent deviations from this tidal trend are small and do not have a specific pattern, indicating that they are not related to the signals of interest contained within the data. The low frequency signal generated by the ships was isolated using a Savitzky-Golay convolution filter (Figure 13). To separate the high frequency signal from the low frequency signal, the Savitsky-Golay filtered data were subtracted from the unfiltered RBR data.

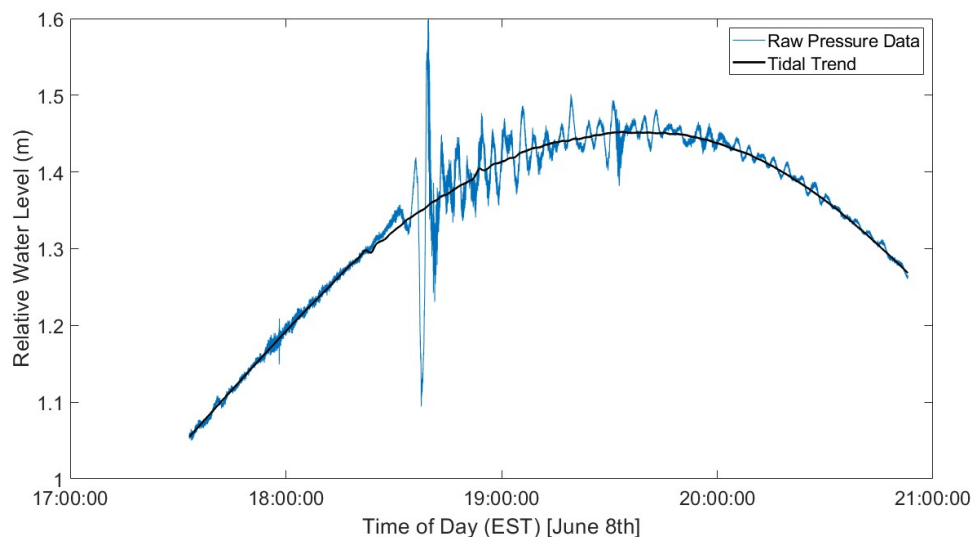


Figure 12 Unfiltered RBR data from the evening on June 8th overlain on the tidal trend that was developed by using a 30-minute moving average.

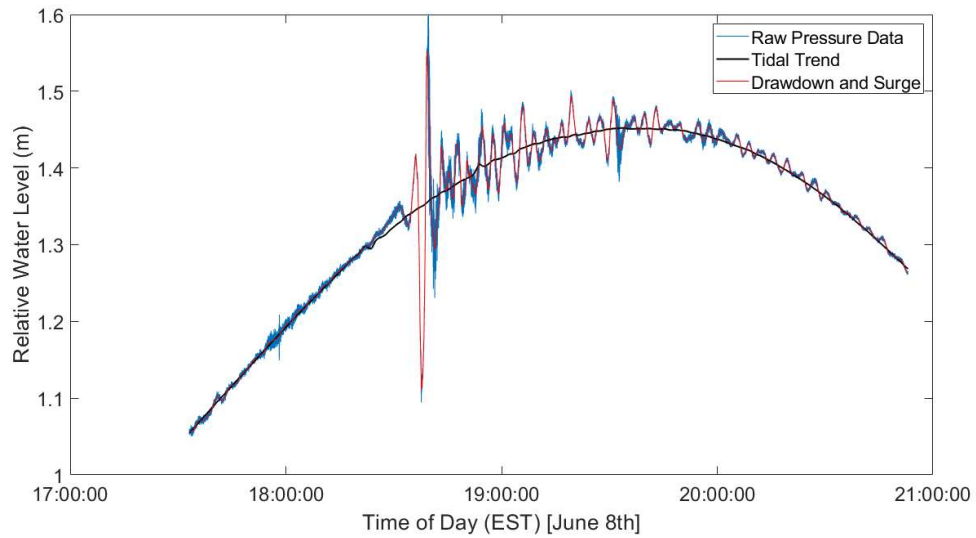


Figure 13 RBR data filtered with a Savitzky-Golay convolution filter plotted with unfiltered RBR data and tidal trend during the evening of June 8th.

The ship wake trains were identified and isolated using their specific low-frequency signal. An algorithm was created to identify the largest local extremum in terms of magnitude for a given frame length that surpassed a minimum absolute prominence threshold within the Savitzky-Golay filtered data. For a valid ship wake this extremum is typically the trough of the drawdown, but in a few rare cases was found to be the crest of the surge. A prominence threshold of 0.05 m was chosen because it was not common for the amplitude of secondary low frequency oscillations following the drawdown and surge to exceed 0.05 m, resulting in false identification or repeat identification of ship wakes (Figure 14). Additionally, ships generating a drawdown or surge with an amplitude less than 0.05 m were determined to produce insubstantial divergent wakes and low energy fluxes.

After a wake was identified, an iterative loop moved the indexed position in the data to the peak water elevation preceding the initial drawdown and a 15-minute window of the data following the index position was retained. The retained data segment was saved to an indexed structure of ship wakes chronologically ordered by when the ship traveled past the island. The 15-minute window was chosen because wave heights beyond 15 minutes contributed to a relatively insignificant energy flux compared to the rest of the wake train. The only remaining wake waves after 15 minutes are low-frequency undulations. The first wave following the 15-minute window has an average height of 0.05 m and an average period of 180.91 s, resulting in a 12.88 N/s, or <1 %, energy flux contribution to the total wake event.

Upon separating the wake trains from the collected data set, the time of passing relative to the inception of data collection was recorded to correlate with time lapse footage and a detailed shipping log of all ships recorded in the Delaware River and Bay during the study. Furthermore, since the pressure sensor at Station M0 was submerged for the greatest length of time during the study, the events obtained from it were counted to quantify the number of events eligible for analysis.

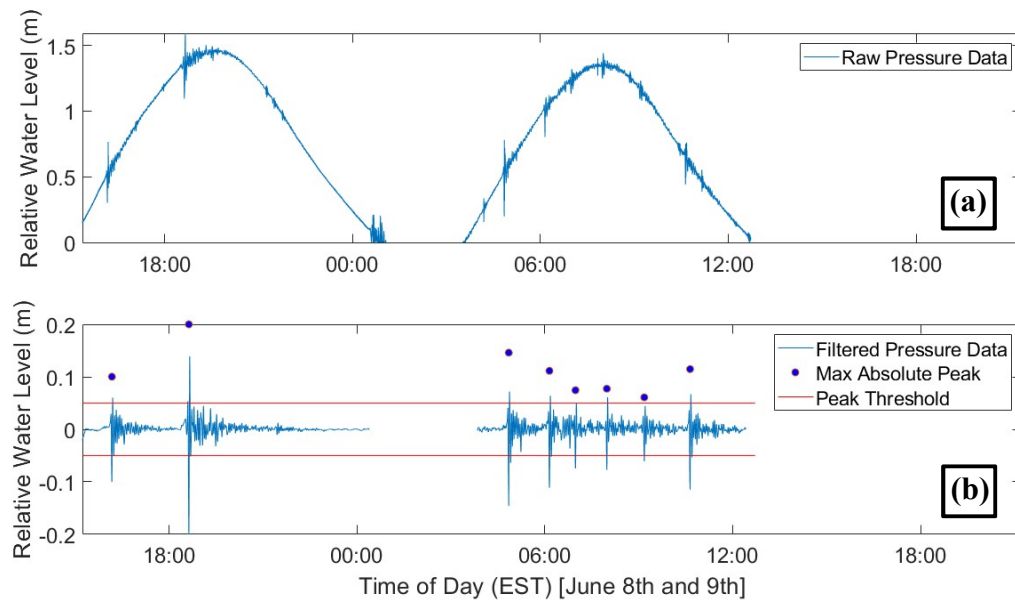


Figure 14 (a) Time series of a 24-hour segment of low frequency filtered data before the tidal trend was removed. (b) Same filtered data with the tidal trend removed and individual event extrema identified (the extrema are plotted in absolute magnitude).

2.2.2.1 Time Series Analysis

To analyze the ship induced wake events, short-term wave analysis was performed for each event. Because the wave fluctuations were already centered around the relative mean water level, the most rational path forward in analyzing the data was to use a time domain analysis rather than converting over to a frequency domain analysis. With tidal trends removed, the wave height can be defined by adding the absolute vertical distance of the maximum and minimum water levels. A practical approach to obtain these maximum and minimum values was proposed by Gharbi et al (2010) to use a zero down crossing method to isolate the individual waves in each shipping wake event. The zero down crossing method works by identifying where the downslope of the wave signal first crosses the x-axis and then each subsequent

downward crossing in the event identifies a wave. It is straightforward to acquire the wave period using this method, by simply finding the temporal distance between each down crossing.

2.2.2.2 Automatic Identification System (AIS) Data

Following the completion of the field study, a shipping log of all large commercial ships that had navigated the Delaware River during the study was provided by the Maritime Exchange for the Delaware River and Bay. The log was generated using the U.S. Coast Guard's AIS data which records ships specifications and time stamps pertaining to each ship when entering a waterway or port. Limiting the log to relevant ship passages was imperative for it to be a practical resource in cross referencing uncertain ship wake data signals that were unable to be verified with the time lapse footage. Approximately 93% of ships entering the Delaware River and Bay system pass through the Breakwater (BW) entrance, and the remaining 7% enter through the Chesapeake and Delaware Canal (CD) port system (Almaz & Altiok, 2012). Both entrances are located south of Pea Patch Island, so all inbound ships must pass the study site if their destinations are farther up river. Likewise, outbound ships departing from ports and anchorages north of the island must also pass by the study site. However, there are instances where ships will access the Chesapeake Bay by way of entering through BW and using the CD Canal, as well as a few ports and anchorages that are located south of the island that ships may be traveling to or from. Additionally, each ship will have at least 3 recordings per visit to the waterway, one upon entry, one for arrival at the port of destination, and one upon exiting the waterway. Often ships will have more than 3, accounting for anchorage stops and lightering locations.

The Actual Time of Arrival (ATA) at the Breakwater entrance to Delaware Bay was correlated with the ATA at each ship's respective destination to confirm each vessel passage by Pea Patch Island. The Breakwater ATA did not include whether the ship is entering or departing Delaware Bay, so prior and posterior ATA's for each vessel were inspected to confirm the direction the ship was traveling and whether it had passed Pea Patch Island. All ships that did not pass Pea Patch Island during the field study were removed from the log, and only the most relevant ATA for each ship that had passed was kept to avoid redundant ship counts. The final product of the reorganized shipping log concluded that 353 ships travelled past Pea Patch Island during the study period. Of the 353 reported by the log, 189 (~54%) generated wakes that met the minimum peak wave height threshold and time parameters to be identified by the RBR at station M0.

Chapter 3

RESULTS

3.1 Wake Characteristics

The data analysis revealed that ships with very large displacements, such as tankers and cargo ships, traveling in a confined waterway produce a consistent signature in terms of wave signal that is unique compared to the wakes generated by other vessels and natural wave conditions (Figure 15). Initially, a slight increase in water elevation travels along with the passing of the ship. This is immediately followed by a substantial drawdown in water level, resulting in an upwelling or surging runup minutes after the ship has passed. The average period of this drawdown and surge effect is approximately 3 to 4 minutes making it a relatively low frequency oscillation compared to other ship induced wakes and meteorologically driven wind waves. Due to the confined nature of a river channel, the drawdown and surge is succeeded by a seiching effect of smaller undulations. These oscillations are small relative to the initial height of the drawdown and surge, but decay thereafter very gradually until the undisturbed water level is met or influenced by another passing ship. This gradual decay in wave height can be attributed to the small frictional forces that are acting upon them (Kamphuis, 2010).

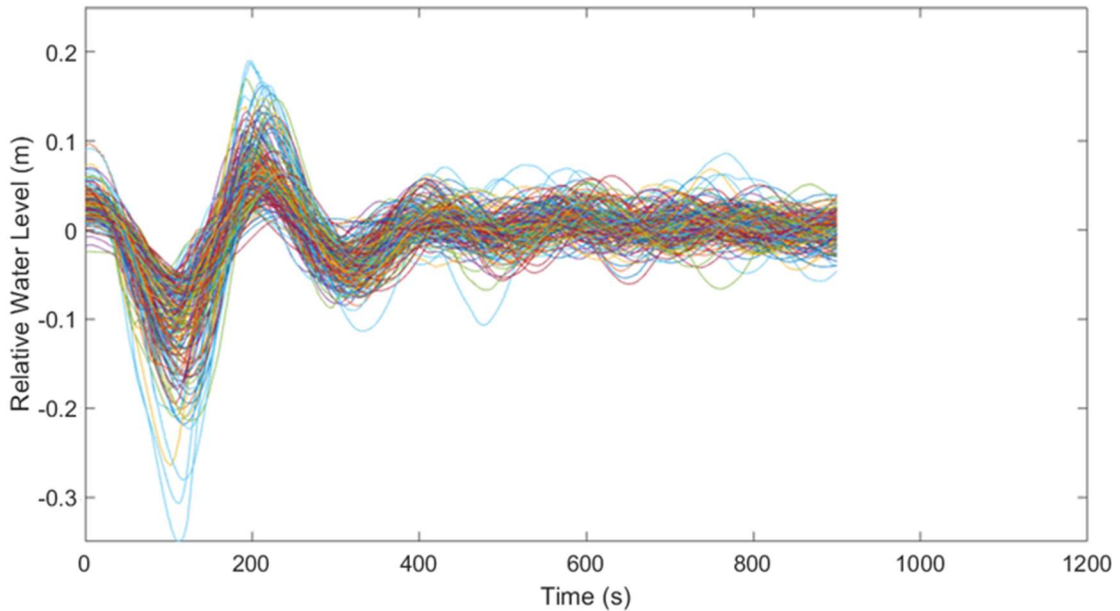


Figure 15 Relative water level plotted over time of low frequency oscillations generated by 189 ships that passed by the study site from June 7th to July 9th.

Although the wave signal is consistent compared to wakes generated from other vessels and natural conditions, there is a subtle variation depending on the direction the ship is traveling in (Figure 16). While the drawdown appears to be consistent in both directions, the surge is limited when the ship is travelling north. This characteristic may be due to the geometry of the river and topographic features of the study site. Ships traveling north past the island generate a surge that propagates alongshore due to the channel running parallel to the beach and a vegetated platform blocking much of the wave's refraction. Whereas the surge generated by ships traveling south past the island propagates at a much smaller incident angle relative to the shore due to a bend in the channel upriver of Pea Patch Island. Considering the unimpeded surge of ships traveling southward, a simple assumption that the surge

would be the direct contrast of the drawdown, however, the drawdown was most commonly greater in magnitude than the incoming surge.

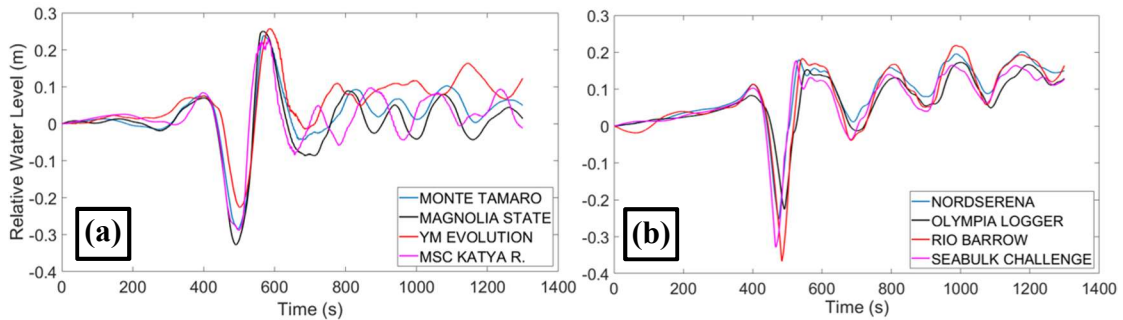


Figure 16 Low frequency signals of 8 ships traveling during a similar tide phase. **(a)** Ships traveling south past Pea Patch Island. **(b)** Ships traveling north past Pea Patch Island.

3.2 Geomorphological Change

Over the course of the project, the meteorological conditions were mild (max wind speed: 11.2 m/s from the NNE, average wind speed: 2.9 m/s from the S as shown in Figure 17) in comparison to the many storms and Nor'easters that batter the Mid Atlantic coast throughout the year. Due to the orientation of the study site, the beach was sheltered from the majority of the aeolian influences which came from the south. Conversely, the strongest aeolian influences came from the north-northeast directly impacting the beach as well as providing the longest fetch for wind wave setup. However, these events were infrequent, and duration limited, making their total contribution to morphological change over the course of the study insignificant. Under these encountered conditions, the beach did not show any discernible change and the

RTK surveys validated this observation by revealing negligible temporal variations along the transect profile (Figure 18).

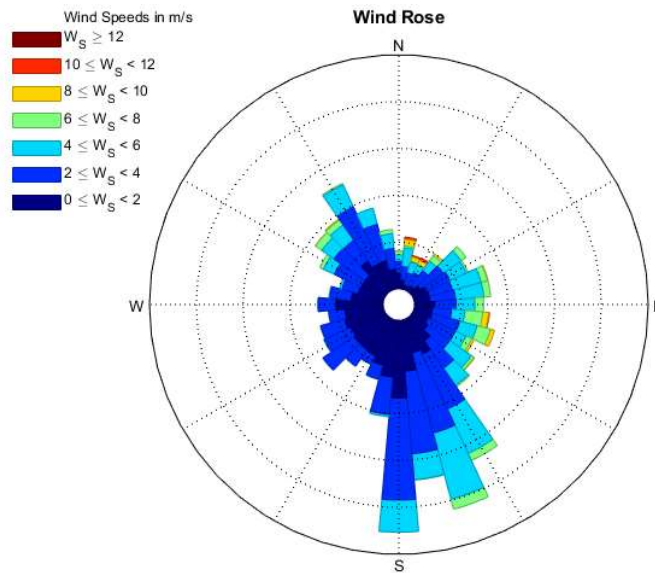


Figure 17 Wind rose of wind speed and direction from June 7, 2018 to July 9, 2018. Data obtained National Data Buoy Center (NDBC) Station DELD1 (Delaware City).

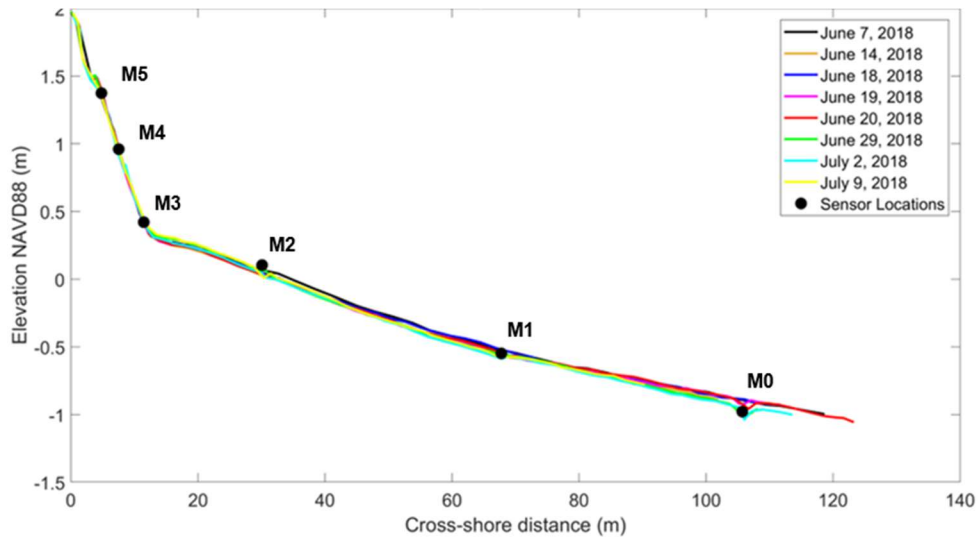


Figure 18 During the field study 8 profile surveys were conducted and plotted together to compare the temporal variations over the duration of the study. The legend identifies the each of the colored curves with the corresponding date of the survey.

The results of profile surveys exhibit a gradual slope in the foreshore region of the beach extending from the toe of the berm to the farthest offshore surveyed location. The high tide line does not extend much farther beyond the toe of berm, so it is expected that much the of the wave breaking at the study site will occur offshore.

3.3 Energy Flux

It is essential to calculate the energy flux generated by the ships traveling past the study site to quantify the impacts of ship wakes, if a device to measure suspended sediment across the transect is not available. The erosion caused by ship wakes and wash is considered proportional to the wave power density, also referred to as the wave energy flux (Gharbi et al., 2010). The energy flux equation is derived from multiplying the wave energy per unit surface area by the unit width of wave crest. The

energy per unit surface area is related to the square of the wave height (H), water density (ρ), and the acceleration of gravity (g)

$$E = \frac{1}{8}\rho gH^2. \quad (3.1)$$

To obtain energy flux, the calculated energy density is multiplied by the velocity of propagation or celerity (C) and the group velocity parameter (n).

$$P = ECn, \quad (3.2)$$

where C and n are determined by

$$C = \frac{gT}{2\pi} \tanh(kd), \quad (3.3)$$

$$n = \frac{1}{2} \left[1 + \frac{2kd}{\sinh(2kd)} \right]. \quad (3.4)$$

In these equations T is the wave period, d is depth, and k is the wave number represented by

$$k = \frac{2\pi}{L}. \quad (3.5)$$

To use these equations effectively, both wave height and wave period needed to be collected from the data obtained during the field study. Height is a much more influential factor in the variation of energy flux because energy flux is a function of the wave height squared and celerity is linearly related to the wave period. Although the contribution of energy is much smaller for waves with a small wave height and short period relative to larger waves within the event, it is important to account for the

energy associated with all the waves considering the overall quantity of small contributions that may occur over the duration of the event. The total energy flux of the event was calculated as a summation of individual waves in both the low- and high-frequency signals. The wake events were then reanalyzed to ensure that only the wakes identified initially at station M0 were calculated across the transect, eliminating the risk of false signals in shallower water that were not detected at M0. The collected contribution of energy fluxes was averaged per day and compared to the daily averaged overall energy experienced across the transect (Figure 19). It is important to note that the overall energy flux imposed on the upper regions of the beach was noticeably smaller than the seaward stations due to tidal influences resulting in varying water depth (Figure 20). The reduced exposure to natural hydrodynamic forces, subsequently reduces the risk of ship induced impacts as well.

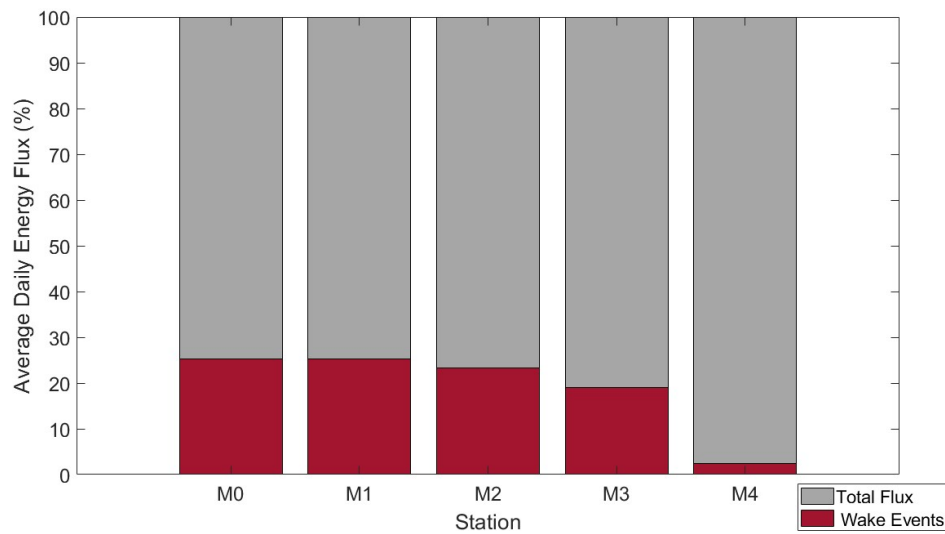


Figure 19 Percent of average daily energy flux contributed by identified ships compared to the total daily energy flux experienced at each station along the transect.

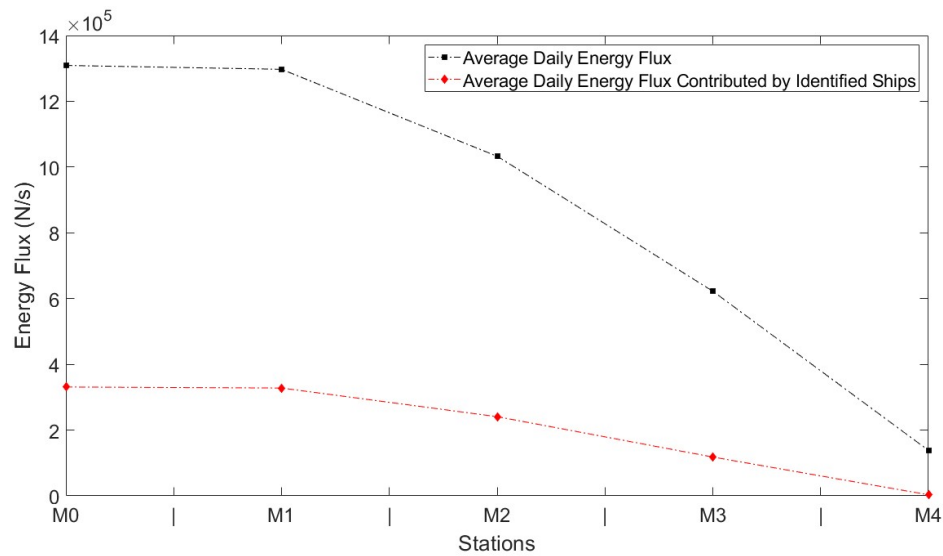


Figure 20 Averaged total daily energy flux recorded at Stations M0 – M4 compared to the averaged daily energy flux contributed by the wake events identified in the RBR pressure data.

The average energy flux per day generated by ships appears small (~25%) in comparison to the average total flux per day, but only an average of 6 ships per day were identified and recorded. At 15 minutes measured per ship wake event, the average generated flux per day consists of only 90 minutes, which is 6.25% of the day. In comparison, the average ambient energy flux over a 15-minute timeframe is approximately 10% of the energy flux generated by a ship wake event (Table 3.1). The ambient energy flux varies substantially with water depth due to wave height's dependence on depth, so the percentage is much greater at lower tides. However, the average is validated because it was found that at high tide the percentage can drop significantly, the magnitude would suggest a factor of ten.

Table 3.1 Average energy flux per ship and average ambient energy flux during a 15-minute period.

Station	Total Identified Wake Events	Number of Wake Events Kept	Average Energy Flux per Ship (N/s)	Average Ambient Energy Flux (N/s)
M0	189	169	1.96E+03	197.06
M1	189	159	2.06E+03	202.37
M2	189	133	1.81E+03	190.12
M3	189	69	1.71E+03	169.45
M4	189	14	2.32E+02	45.37

If the ship wake energy fluxes are examined individually, without averaging, the dissipative pattern is still evident, yet an increase in the energy flux is observed as the waves reach their respective breaker depth (Figure 21). As conditions become more dissipative, wave asymmetry increases with wave height increasing and wave length decreasing (Houser, 2011). Once the wave has reached its critical steepness, it will break and dissipate its energy as shown at station M3 in Figure 21. The period of the waves should remain constant based on small amplitude wave theory which implies that the same number of waves are contributing to the total energy flux of the wake train (Kamphuis, 2010). The calculation of energy flux in this project is based off the highly simplified assumption that the wave spectra is two dimensional and unidirectional, propagating normal to the shoreline. There are reflected waves propagating undissipated energy offshore as well as angular wave energy contributions that cannot be delineated using hydrostatic pressure measurements alone. The additional disregarded energy contributions are likely the cause of increased energy flux levels exhibited in Figure 21.

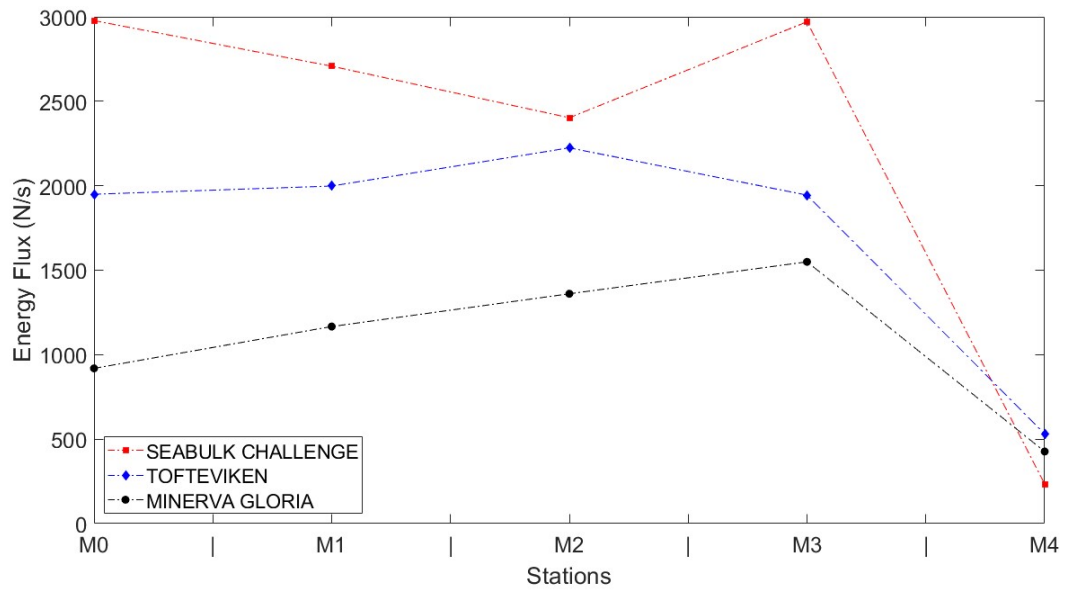


Figure 21 Energy Flux recorded across the transect of 3 randomly selected ships. An increase in energy flux can be observed as the waves move landward toward shallower water and then rapidly dissipate after breaking.

Chapter 4

CONCLUSIONS AND FUTURE WORK

Although the energy flux contained within the wake train generated by large ships is large relative to the energy flux generated by ambient river conditions during the wake event, the average energy flux impacting the island over the course of a day is only about 25% of the overall energy flux contributed by calm meteorological conditions. The addition of larger ships and greater shipping traffic density will drastically increase the amount of energy that Pea Patch Island must dissipate daily. Even just an increase from 6 to 10 ships in a day generating the same amount of energy per ship will increase the ship induced energy flux contribution to ~50%. In addition to larger ships and greater shipping traffic density, less ships will need to be lightered to travel upstream. This will result in larger hull displacements generating greater transverse waves that could overtop the already threatened beach.

The results have shown that the study site was well defended against the impeding waves in that there was substantial dissipation of energy as the waves propagated across the transect. It is worth noting, the most accurate means of determining energy dissipation with the collected data is to compare the gradient in energy flux between stations during the same wake event. Additionally, the most conclusive findings can be obtained during a high tide when the majority of sensors are submerged and there is a smaller risk of gaps in the data due to low water levels. During the majority of the tidal cycle, the water level was below the base of the berm. This region of the beach had a gradual slope, resulting in longer exposure to bottom frictional forces and increasing the offshore breaker distance for larger waves (Iribarren and Nogales, 1949).

The direct impact of the energy flux calculations is dependent on the specific gravity of the sediment and the incident wave angle. This study was unable to measure the incident wave angle, so radiation stresses could not be obtained. Future work can include measuring suspended sediment during a ship wake event to delineate the proportional relationship between the energy fluxes and induced sediment transport. Furthermore, ship wake induced energy fluxes should be measured against varying weather conditions to fully understand the coupled effect of constructive interference with higher tides and meteorological waves. Conducting additional data collection during other periods of the year as well a long-term profile study can provide stronger evidence of temporal variability in the geomorphological effects of shipping traffic on Pea Patch Island.

REFERENCES

- Almaz, O. A., & Altiok, T. (2012). Simulation modeling of the vessel traffic in Delaware River: Impact of deepening on port performance. *Simulation Modelling Practice and Theory: International Journal of the Federation of European Simulation Societies*, 22, 146–166.
- Cook, T. L., Sommerfield, C. K., & Wong, K. C. (2007). Observations of tidal and springtime sediment transport in the upper Delaware Estuary. *Estuarine, Coastal and Shelf Science*, 72(1-2), 235-246.
- Gharbi, S., Valkov, G., Hamdi, S., & Nistor, I. (2010). Numerical and field study of ship-induced waves along the St. Lawrence Waterway, Canada. *Natural Hazards*, 54(3), 605–621. <https://doi.org/10.1007/s11069-009-9489-6>
- Houser, C. (2011). Sediment Resuspension by Vessel-Generated Waves along the Savannah River, Georgia. *Journal of Waterway, Port, Coastal, and Ocean Engineering*, 137(5), 246–257. [https://doi.org/10.1061/\(ASCE\)WW.1943-5460.0000088](https://doi.org/10.1061/(ASCE)WW.1943-5460.0000088)
- Iribarren, C. R., & Nogales, C. (1949). Protection des ports, paper presented at xviith international navigation congress, permanent int. *Assoc. of Navig. Congr.*, Lisbon, Portugal.
- Kamphuis, J. W. (2010). *Introduction to Coastal Engineering and Management*. World Scientific.
- Kjerfve, B. (2018). *Hydrodynamics of Estuaries: Volume II Estuarine Case Studies*. CRC Press.

Komar, P. D. (1998). *Beach processes and sedimentation*. Upper Saddle River, N.J.:
Prentice Hall.

Parker, B. B. (1984). *Frictional effects on the tidal dynamics of a shallow estuary*.

Retrieved from <http://catalog.hathitrust.org/api/volumes/oclc/69954913.html>

Ross, A. C., Najjar, R. G., Li, M., Lee, S. B., Zhang, F., & Liu, W. (2017).

Fingerprints of Sea Level Rise on Changing Tides in the Chesapeake and

Delaware Bays. *Journal of Geophysical Research: Oceans*, 122(10), 8102–

8125. <https://doi.org/10.1002/2017JC012887>